

PROCEEDINGS

Nineteenth International Tissue Elasticity Conference

Seattle, WA, USA

June 26th – 29th, 2025



The leader in Research Ultrasound™

FUJIFILM
VISUALSONICS

vermon

SONIC™
CONCEPTS



YESWEHAVE®
OCT Components & RGB Laser

Seattle, WA, USA, June 26th – 29th, 2025

Contents

Sponsors.....	3
Conference Venue.....	7
Organizing committee.....	8
Detailed program.....	9
Session Chairs.....	9
Thursday, June 26 th	10
Friday, June 27 th	11
Saturday, June 28 th	12
Special Events & Highlights.....	14
Abstracts.....	15
Thursday, June 26 th	15
Friday, June 27 th	25
Saturday, June 28 th	31



Expanding Ultrasound Research



Vantage[®] **NXT** Research Ultrasound System

- Accelerate research
- Simplify data collection and analysis
- Real-time access to receive data on every channel
- Frequency range options from 20 kHz - 60 MHz
- Platform upgradability protects capital investments

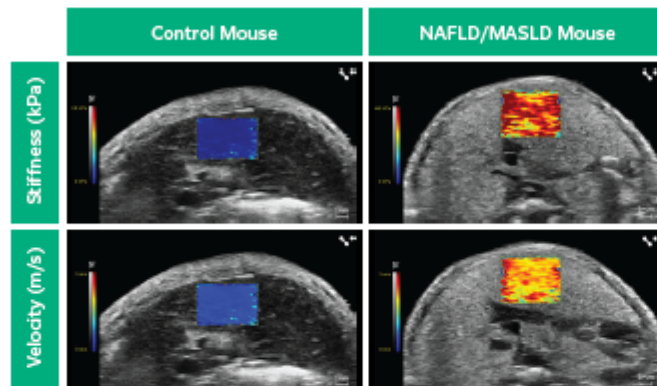
Verasonics Inc.
11335 NE 122nd Way, Suite 100, Kirkland, WA 98034
www.verasonics.com



Learn more or E-mail:
sales@verasonics.com

Unlock Tissue Stiffness with Precision

Advanced Shear Wave Elastography on the Vevo F2 Ultrasound Platform



Shear Wave Elastography (SWE)

on the Vevo F2 Imaging system offers unparalleled sensitivity for assessing tissue stiffness in small animal models.



Scan the QR code

to learn more about shear wave elastography on our website.

KEY FEATURES

Fully Integrated on Vevo F2

Seamless integration for enhanced workflow allowing users to select 4 or 2 push pulses and easily manipulate data display.

Quantitative Analysis & Quality Display Map

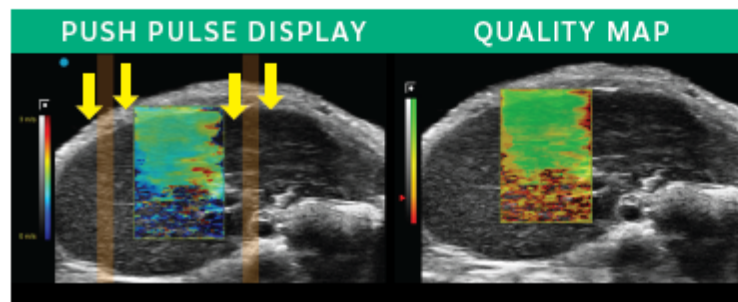
Measure shear wave velocity and stiffness in kPa for precise assessment; a quality display map provides insight into data acquisition quality.

Real-time Visualization

Superimposed, real-time data display maps onto anatomical images for comprehensive analysis.

Optimized for Small Animal Models

Tailored for high-resolution imaging of small animal tissues.

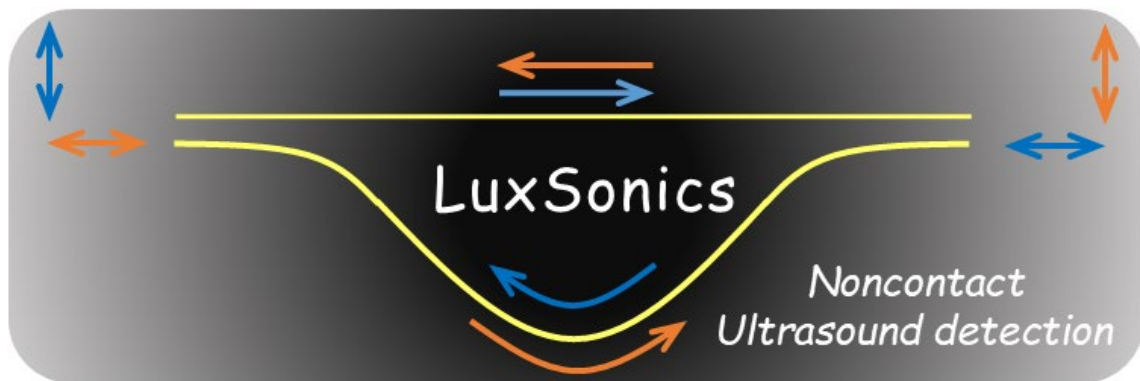


vermon

Custom Ultrasound Probes
and Transducers



vermon.com

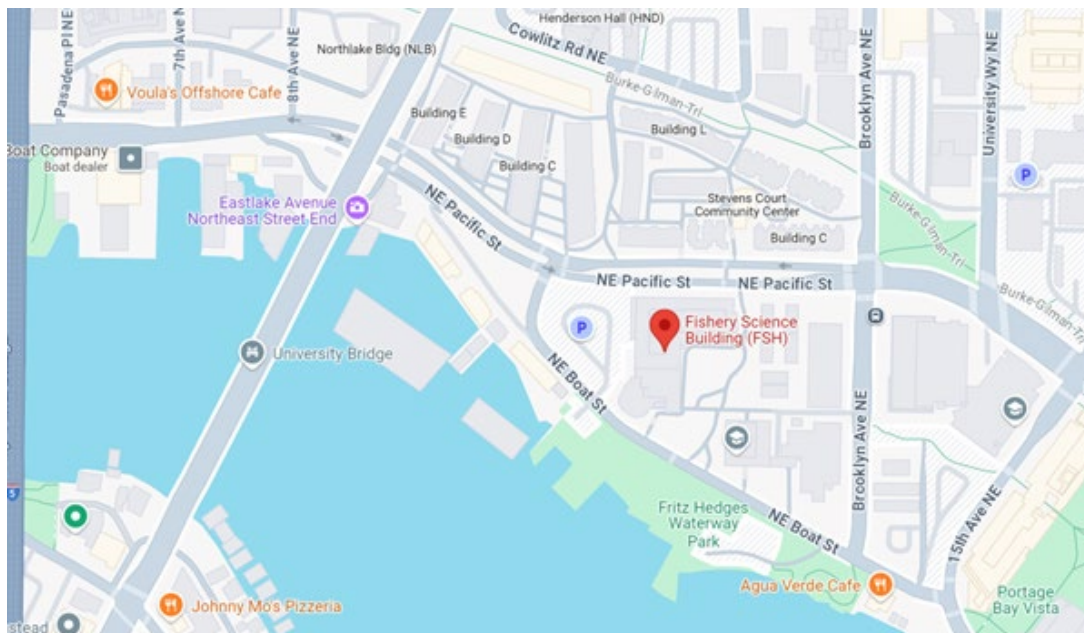


YESWEHAVE[®]
OCT Components & RGB Laser

SONIC[™]
C O N C E P T S

Conference Venue

University of Washington, Fishery Science bld., #102
1122 NE Boat Street, Seattle, WA 98195, USA



Organizing Committee

Chair

Stefan Catheline

LabTAU, INSERM, Centre Léon Bérard, Université Claude Bernard Lyon 1, Lyon, France

Secretary

Jorge Torres

LabTAU, INSERM, Centre Léon Bérard, Université Claude Bernard Lyon 1, Lyon, France

Treasurer

Bruno Giammarinaro

LabTAU, INSERM, Centre Léon Bérard, Université Claude Bernard Lyon 1, Lyon, France

Chair of ITEC 2025

Ivan (Vanya) Pelivanov

University of Washington, Department of Bioengineering, Seattle, WA, USA

Consultants

Jeffrey Bamber

Institute of Cancer Research, UK

Mathias Fink

Institut Langevin, ESPCI ParisTech, PSL University, France

Detailed program

Session chairs

Plenary I Thursday, 9:15–10:00	Kirill Larin
OPM I (Optical Methods in Elastography I) Thursday, 10:30–12:00	Kirill Larin, Vanya Pelivanov
Plenary II Thursday, 13:55–14:40	Ricky Wang
OPM II (Optical Methods in Elastography I) Thursday, 14:40–16:00	Matt O'Donnell
USM I (Ultrasound Methods in Elastography I) Friday, 8:50–10:40	Tatiana Khokhlova, Thomas Royston
Industry Friday, 11:00–12:30	Stefan Catheline
Keynote Saturday, 9:00–9:40	Bruno Giammarinaro
MRM (Magnetic Resonance Methods in Elastography) Saturday, 9:40–10:40	Ingolf Sack
USM II (Ultrasound Methods in Elastography II) Saturday, 11:00–12:30	Ricardo Andrade, Salavat Aglyamov
USM III (Ultrasound Methods in Elastography III) Saturday, 14:00–15:40	Jorge Torres
USM IV (Ultrasound Methods in Elastography IV) Saturday, 16:10–17:20	Stefan Catheline, Ginger Schmidt

Thursday, June 26th

8:00–9:00	Registration		
9:00–9:15		WELCOME SESSION	
9:15–10:00	PL	Ricky Wang Plenary	RECENT DEVELOPMENT IN OPTICAL COHERENCE TOMOGRAPHY AND ELASTOGRAPHY
10:00–10:30	Coffee break		
10:30–11:00	IT	Matt O'Donnell University of Washington, USA	COORDINATE-INDEPENDENT 3-D ULTRASOUND PRINCIPAL STRETCH AND DIRECTION IMAGING FOR CARDIAC STRAIN IMAGING
11:00–11:20	OPMI	Salavat Aglyamov University of Houston, USA	ELASTICITY IMAGING OF THE OCULAR LENS USING ACOUSTIC RADIATION FORCE
11:20–11:40	OPMI	Ginger Schmidt Harvard Medical School and Massachusetts General Hospital, USA	ELASTICITY MEASUREMENT OF THE HUMAN CORNEA IN VIVO WITH 3D ASYNCHRONOUS OPTICAL COHERENCE ELASTOGRAPHY (ASYNCOE)
11:40–12:00	OPMI	Bruno Giammarinaro LabTAU, France	ELASTIC WAVES IN VISCOELASTIC SOFT STRINGS REVEALED BY OPTICAL ELASTOGRAPHY
12:00–13:55	Lunch		
13:55–14:40	PL	Kirill Larin Plenary	RECENT DEVELOPMENT IN OPTICAL COHERENCE TOMOGRAPHY AND ELASTOGRAPHY
14:40–15:00	OP-MII	Agathe Marmin University of Washington, USA	ROBOTIC MULTIMODAL OCT/OCE ON SKIN IN-VIVO: INITIAL CONCLUSIONS
15:00–15:20	OP-MII	Shyamal Guchhait University of Washington, USA	RECONSTRUCTING ANISOTROPIC MECHANICAL MODULI IN SKIN FROM NON-CONTACT DYNAMIC OPTICAL COHERENCE ELASTOGRAPHY
15:20–15:40	OP-MII	Malauri Devissi LabTAU, France	STUDY AND RECONSTRUCTION OF THE MECHANICAL ENDOMETRIAL TUMOR MICROENVIRONMENT USING MICROELASTOGRAPHY
15:40–16:00	OP-MII	Stefan Catheline LabTAU, France	GRAVITATIONAL LENS EFFECT IN A SOFT FABRIC MEMBRANE
16:00–16:30	Group photo and coffee break		
16:30–18:30	University of Washington Lab Tour		
18:30–22:00	Welcome aperitif		

Friday, June 27th

8:30–8:50		ANNOUNCEMENTS	
8:50–9:20	IT	Stefan Catheline LabTAU, France	UNVEILING TISSUE SECRET USING VIBRATIONS
9:20–9:40	USM I	Tatiana Khokhlova University of Washington, USA	ELASTICITY MAPPING WITH HIGH INTENSITY FOCUSED ULTRASOUND FOR PROSTATE ABLATION TREATMENT PLANNING
09:40–10:00	USM I	Axel Nierding Université Paris Saclay - CNRS, France	DIAPHRAGM LOADING INDUCED CHANGES IN SHEAR MODULUS AS ASSESSED WITH ULTRASOUND SHEAR WAVE ELASTOGRAPHY IN ABSENCE OF DETECTABLE CONTRACTILE FATIGUE
10:00–10:20	USM I	Haokang Shi Columbia University, USA	PULSE WAVE IMAGING FOR EARLY-STAGE ATHEROSCLEROSIS MONITORING AND DETECTION: A PRELIMINARY STUDY IN HYPERCHOLESTEROLEMIC SWINE MODEL
10:20–10:40	USM I	Hossein Aghamiry Charité - Universitätsmedizin, Germany	ULTRASOUND TIME-HARMONIC ELASTOGRAPHY FOR THE ASSESSMENT OF INDUCED MUSCLE STIFFNESS IN RESPONSE OF TONIC VIBRATION REFLEX
10:40–11:00	Coffee break		
11:00–11:30	IT	VERASONICS	
11:30–11:50	IT	VISUALSONICS	
11:50–12:10	IT	SONIC CONCEPTS	
12:10–12:30	IT	VERMON	
12:30–14:00	Lunch		
14:00–18:00		TOURS TO COMPANIES	
18:30–23:00	SOCIAL EVENT: DINNER		

Saturday, June 28th

8:50–9:00		ANNOUNCEMENTS	
9:00–9:40	KN	Ingolf Sack Charité - Universitätsmedizin, Germany	MULTI-FREQUENCY TIME HARMONIC ELASTOGRAPHY ACROSS SCALES, DYNAMICS, AND PLATFORMS
9:40–10:00	MRM	Noah Jaitner Charité - Universitätsmedizin, Germany	COMBINED MR ELASTOGRAPHY AND 3D MRI DEFORMATION MAPPING TOWARDS IN VIVO ASSESSMENT OF SOLID STRESS IN GLIOBLASTOMA
10:00–10:20	MRM	Biru Huang Charité - Universitätsmedizin, Germany	ASSOCIATION OF GUT MICROBIOME WITH MASLD AND MASH AND ITS CORRELATION WITH MR ELASTOGRAPHY IN MICE
10:20–10:40	MRM	Biru Huang Charité - Universitätsmedizin, Germany	AN ELASTOGRAPHIC ATLAS OF THE AGING MOUSE BRAIN
10:40–11:10	Coffee break		
11:10–11:30	USM II	Ryan Pitsinger NC State University, USA	MULTI-PLANE SHEAR WAVE ELASTOGRAPHY: TOWARDS 3D IMAGING OF TISSUE VISCOELASTICITY
11:30–11:50	USM II	Yangpei Liu Columbia University, USA	3-D IMPLEMENTATION OF SINGLE TRANSDUCER-HARMONIC MOTION IMAGING USING A ROW-COLUMN-ADDRESSED (RCA) ARRAY
11:50–12:10	USM II	Xin Sun University of Southern California, USA	Four-Dimensional (4D) Ultrasound Shear Wave Elastography Using Sequential Excitation
12:10–12:30	USM II	Joaquin Mura Universidad Tecnica Federico Santa Maria, Chile	A MULTIGRID SCHEME FOR EFFICIENT INVERSION USING A FINITE-VOLUME METHOD
12:30–14:00	Lunch		
14:00–14:30	IT	Ricardo Andrade Nantes Université, France	MECHANICAL CHARACTERIZATION OF TRANSVERSE ISOTROPY IN NEUROMUSCULAR TISSUES
14:40–15:00	USM III	Kaden Bock Duke University, USA	OPTIMIZING MULTI-MODALITY ANISOTROPIC ELASTICITY IMAGING PHANTOMS
15:00–15:20	USM III	Wren Wightman Duke University, USA	ON THE STABILITY OF TIME-OF-FLIGHT-BASED SHEAR WAVE SPEED ESTIMATORS USING SLOWNESS AND VELOCITY
15:20–15:40	USM III	Thomas Royston University of Illinois Chicago, USA	ELASTOGRAPHY IN PRESTRESSED AND TRANSVERSELY ISOTROPIC VISCOELASTIC STRUCTURES: INVERSE MODELING CHALLENGES

15:40–16:10	Coffee break		
16:10–16:40	IT	Vanya Pelivanov University of Washington, USA	QUANTITATIVE RESOLUTION OF DYNAMIC OCE IN THE CORNEA: CAN WAVE GUIDANCE BE OVERCOME?
16:40–17:00	USM IV	Enrique Gonzalez-Mateo Universitat Politècnica de València, Spain	IMPROVING SHEAR WAVE ELASTOGRAPHY BY CODED ACOUSTIC RADIATION FORCE
17:00–17:20	USM IV	Mareike Wolff Charité – Universitätsmedizin Germany	ULTRASOUND TIME-HARMONIC ELASTOGRAPHY IN ADULT ZEBRAFISH
17:20–17:50	Student Awards and Closing Session		

Sunday, June 29th

FULL DAY	SOCIAL EVENT
----------	--------------

Special Events & Highlights

Thursday, June 26th 16:00	ITEC 2025 Group Photo Lobby, Fishery Science bld.
Thursday, June 26th 18:30 – 22:00	ITEC 2025 Reception Lobby & Lawn, Fishery Science bld.
Friday, June 27th 14:10 – 17:00 Sign up in the Lobby till Thursday noon	Tour to Sonic Concepts Leaving Fishery Science bld. at 14:10, arrive back by about 17:00.
Friday, June 27th 18:30 – 23:00	ITEC 2025 Dinner 824 NE 102 Street, Seattle, WA 98125
Saturday, June 28th 17:20 – 17:50	Student Award and Closing Session
Sunday, June 29th 7:30 am – full day Sign up in the Lobby till Thursday noon	Mt. Rainier Hiking Tour Leaving Fishery Science bld. at 7:30 am, full day expected.

Abstracts



Thursday, June 26th

Recent Development in Optical Coherence Tomography and Elastography

Ruikang (Ricky) Wang¹ and Kirill V. Larin²

¹University of Washington, Department of Biomedical Engineering, USA

²University of Houston, Department of Biomedical Engineering, USA

Optical coherence tomography (OCT) has revolutionized imaging in many biomedical applications, offering micrometer-level resolution in three dimensions and non-invasive insights into biological tissues. In this talk, we will delve into the latest advancements in OCT technology and many basic science and clinical applications. Special focus will be given to two functional extensions of OCT: OCT-based Angiography (OCTA) and Optical Coherence Elastography (OCE). We will discuss their applications in ophthalmology, oncology, and developmental biology, emphasizing the integration of these technologies for comprehensive diagnostics. Finally, we will highlight several key advantages and limitations of OCT, OCTA, and OCE and provide perspectives on likely future advances and opportunities in these fields.

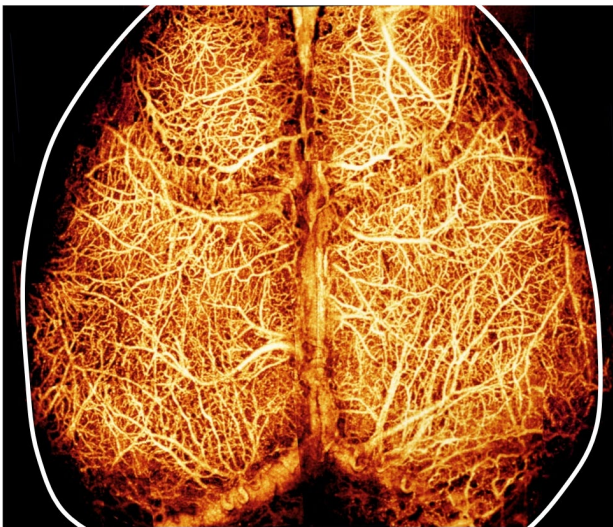


Figure 1. In vivo OCT angiography of the brain cortex in a mouse model, showing microvascular structures at capillary resolution.

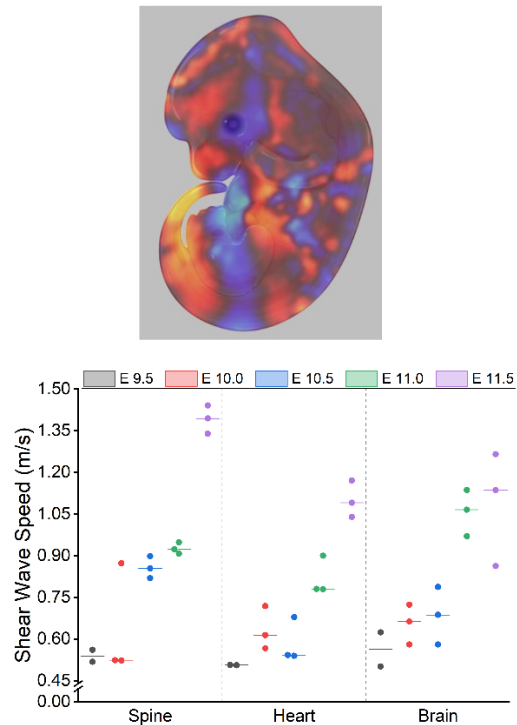


Figure 2. (top) Illustration of reverberant shear wave field generated in a mouse embryo and (bottom) quantification of the shear wave speed across different organs and embryonic development.

Coordinate-Independent 3-D Ultrasound Principal Stretch and Direction Imaging for Cardiac Strain Imaging

Matthew O'Donnell¹, Geng-Shi Jeng²

¹ University of Washington, Department of Bioengineering, Seattle, USA

² National Yang Ming Chiao Tung University, Institute of Electronics, Hsinchu, Taiwan

Background, Motivation and Objective

In clinical ultrasound, current 2-D strain imaging cannot fully present three orthogonal normal strain components. Most systems also lack shear strain information, as displaying all components is hard to interpret. Here we propose 3-D, high-spatial-resolution, coordinate-independent strain imaging based on principal stretch and axis estimation. All strain components are transformed into three principal stretches along three normal principal axes, enabling direct visualization of the primary deformation

Statement of Contribution/Methods

We devised an efficient 3-D speckle tracking method with tilt filtering, incorporating randomized searching in a two-pass tracking framework and rotating the phase of the 3-D correlation function for robust filtering. This approach significantly improves estimates of axial displacement gradients. Non-axial gradients are estimated by a correlation-weighted least-squares fit constrained by tissue incompressibility.

Results/Discussion

Simulated and in vivo canine cardiac datasets were evaluated to estimate Lagrangian strains from end-diastole to end-systole. The proposed speckle tracking method improves displacement estimation by a factor of 4.3 to 10.5 over conventional 1-pass processing. Maximum principal axis/direction imaging enables better detection of local disease regions than conventional strain imaging, as illustrated below.

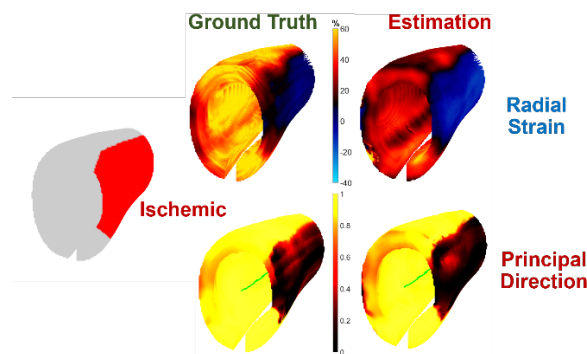


Figure 1. Ultrasound 3-D cardiac strain imaging using novel principal directions provides more robust, high-resolution detection of ischemic regions than traditional radial strain imaging.

Conclusions

Coordinate-independent tracking can identify myocardial abnormalities with high accuracy and enhance robustness in cardiac strain imaging.

Elasticity Imaging of the Ocular Lens Using Acoustic Radiation Force

Salavat R. Aglyamov and Kirill V. Larin¹

University of Houston, Department of Biomedical Engineering, Houston, Texas, USA

Background, Motivation and Objective

Mechanical properties of the ocular lens are critical for human vision. The progression of degenerative eye conditions such as presbyopia and cataract is closely linked to the stiffening of the crystalline lens. Comprehensive understanding of lens biomechanics requires a noninvasive technique for *in vivo* measurement of lens mechanical properties. Acoustic radiation force (ARF) offers a promising approach for inducing mechanical deformation. This study aims to explore various aspects of ARF-based lens elastography and develop noninvasive methods for measuring lens biomechanics *in vivo*.

Statement of Contribution/Methods

In this study, we review our recent advancements in lens elastography using ARF to induce dynamic lens deformation and measure displacement and elastic wave propagation on the lens surface with phase-sensitive Optical Coherence Tomography (OCT). This approach was tested *ex vivo* on fresh rabbit and porcine eyeballs. ARF was applied to the lens surface using single-element ultrasound transducers operating at a central frequency of 3.5 MHz. A custom-built closed-loop intraocular pressure (IOP) control system was used to regulate pressure within the eye globes. Measurements were conducted on lenses of different ages, under varying IOP conditions, and in models simulating cataracts. The crystalline lens was exposed to different radiation power levels to evaluate its structural integrity and functional response, ensuring the safety of ARF-based elastography for potential clinical translation. Additionally, a novel noncontact approach utilizing an air-coupled ultrasound transducer—eliminating the need for coupling media or physical contact—was explored and tested.

Results/Discussion

In situ measurements revealed an approximately threefold increase in elastic modulus in mature rabbit lenses compared to young lenses. We also demonstrated that lens stiffness increases with rising IOP. However, elastography measurements indicated that changes in lenticular stiffness due to elevated IOP are significantly less pronounced than those observed in other ocular tissues, such as the cornea and sclera. Our findings showed that cataract formation has a substantial impact on lens biomechanics, leading to increased stiffness. We also demonstrated that surface waves in the lens can be generated within the FDA safety limits for medical ultrasound.

Conclusions

These findings demonstrate the significant potential of ARF elastography for safe and effective clinical translation, enabling the quantitative assessment of lens mechanical properties in relation to age, IOP, and cataract formation.

This study was supported by the National Institute of Health grant EY022362.

Elasticity Measurement of the Human Cornea *in vivo* with 3D Asynchronous Optical Coherence Elastography (AsyncOCE)

Ginger Schmidt^{1,2}, David Veyssset¹, Calvin Smith¹, Brett E. Bouma^{1,2}, Néstor Uribe-Patarroyo¹

¹ Harvard Medical School and Massachusetts General Hospital, Wellman Center for Photomedicine, Boston, Massachusetts 02114, USA

² Massachusetts Institute of Technology, Institute for Medical Engineering and Science, Cambridge, Massachusetts, 02139, USA

Background, Motivation and Objective

Optical coherence elastography (OCE) measures elastic properties with OCT by analyzing the size and speed of shear waves in tissue. However, current methods are limited by slow image acquisition, sensitivity to motion or expensive custom hardware. Our objective is to eliminate these limitations so OCE can be used to help physicians everywhere better diagnose, treat, and monitor pathologies of the cornea.

Statement of Contribution/Methods

In this work, we present AsyncOCE, for the rapid and asynchronous acquisition of 3D shear wave fields. AsyncOCE is compatible with conventional acquisition rates and is based on pairs of B-scans as in angiography. These characteristics drastically reduce sensitivity to motion and increase acquisition speed, even with fine transverse sampling which enables the use of advanced motion correction techniques.

Results/Discussion

We validated the technique by comparing the shear wave fields measured with both AsyncOCE and conventional phase-locked imaging. We demonstrated successful excitation of shear waves via indirect contact through the eyelid. These innovations enabled AsyncOCE measurements in 3 human subjects *in vivo*. Each subject had 4 AsyncOCE measurements in each eye, for a total of 8 per person. We measured sufficient shear wave signal-to-noise ratio up to 2,115 Hz excitation frequency across all subjects.

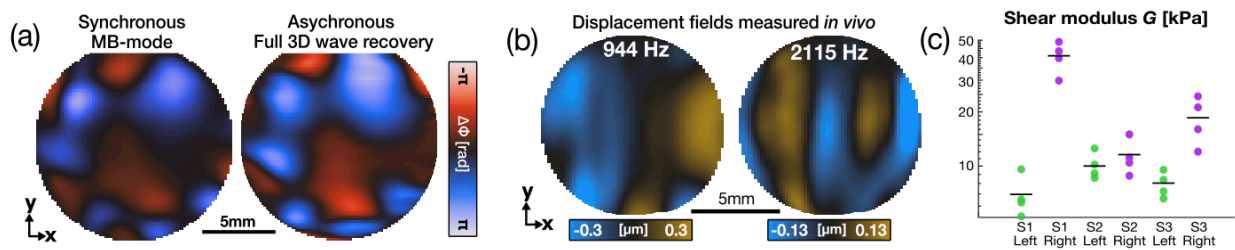


Figure 1. a) Synchronous vs asynchronous methods. b) Shear wave excitation in human subjects was performed through the eyelid, avoiding contact. Waves are not nicely aligned, which necessitated phase gradients for wave number retrieval. c) Multiple measurements acquired from 3 subjects.

Conclusions

AsyncOCE enables rapid and robust measurements of fully coherent 3D shear wave displacement fields in human subjects *in vivo*. We also used an autocorrelation-based phase gradient method for shear wave number retrieval, which is insensitive to the makeup of the shear wave field.

Novel Hybrid Flexural-String Wave Model in Viscoelastic Soft Strings Revealed by Optical Elastography Imaging

J. Zhu¹, S. Grégoire¹, J. Torres¹, F. Turquier², S. Catheline¹, B. Giammarinaro¹

¹LabTAU, INSERM, Centre Léon Bérard, Université Claude Bernard Lyon 1, LYON, France

²Laboratoire de Biomécanique Appliquée, Université Gustave Eiffel/Aix-Marseille Université

Background, Motivation and Objective

Wave propagation in elastic structures is typically described by either string theory (tension-dominated) or beam theory (bending-dominated). However, for soft elastic strings, both effects play a crucial role, making traditional models insufficient. We experimentally studied bending waves in a soft string under varying tensions and developed a unified simplest bending-tension wave model. This research is motivated by potential applications in biological tissues like tendons and ligaments.

Statement of Contribution/Methods

Experiments were conducted on an Ecoflex™ 00-20 FAST soft string with varying tensions, where a mechanical vibrator excited transverse wave. A high-speed camera captured the wave motion, and MATLAB-based image-processing and noise-correlation algorithms extracted wave speeds. We compared these with theoretical predictions and formulated a modified Timoshenko model integrating bending and tension effects.

Results/Discussion

Bending waves were successfully observed, and dispersion curves were extracted under different tensions. The wave speed was highly sensitive to tension, approaching a constant value at low frequencies as tension increased. Neither pure string nor beam theory fully explained the results, but our tension-Timoshenko model closely matched experimental dispersion curves.

Conclusions

Optical imaging enabled precise measurement of bending waves in a tensioned soft string, revealing the coexistence of string and bending waves. Our new model integrates both effects, offering improved wave predictions compared to classical theories. This research benefits applications in biomechanics, but future studies must consider nonlinearities like viscoelasticity for more complex elastic structures.

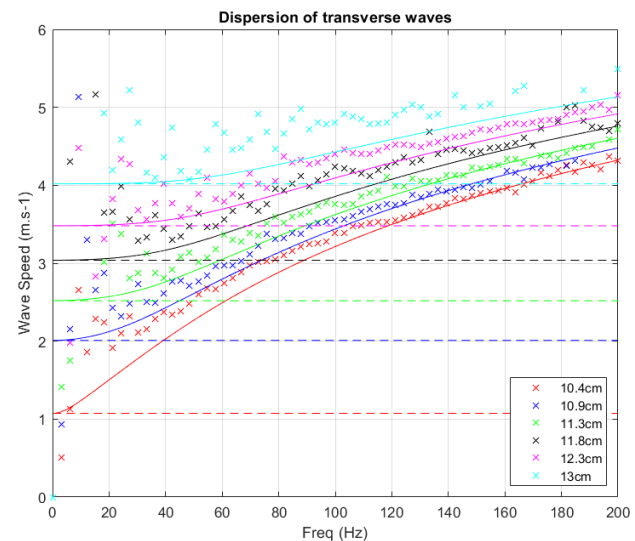


Figure 1. The dispersion curve of transverse wave under different tensions, where the cross points present the experimental data, dash point lines present string wave velocity, solid lines present the tension-Timoshenko string model.

Robotic Multimodal OCT/OCE on Skin *in-vivo*: Initial Conclusions

Agathe Marmin¹, Raveeraj Bawornkitchaikul¹, Clayton Ellington¹, Tam Pham², Russell Ettinger², Matthew O'Donnell¹, Ruikang K. Wang¹ and Ivan (Vanya) Pelivanov¹

¹Department of Bioengineering, University of Washington, Seattle, USA

²Harborview Medical Center, University of Washington, Seattle, USA

Background, Motivation and Objective

Transient optical coherence elastography (OCE) uses the phase sensitivity of motion to detect propagating mechanical waves. This noncontact technique offers stiffness measurements in anterior organs such as skin and ocular tissues. Integrating multiple OCT modalities enhances the ability to study both structural and functional tissue properties.

Statement of Contribution/Methods

This study presents a robotic system designed for noncontact monitoring of skin elasticity, integrating four OCT modalities: structural OCT, polarization-sensitive OCT (PS-OCT), OCT angiography (OCTA), and OCE. An air-coupled acoustic micro-tapping transducer is used to launch plane surface waves over the skin surface. The robotic arm aligns the imaging head and compensates for tissue motion at varying wave propagating directions. Mechanical moduli of skin are reconstructed by fitting the phase velocity angular dependence with a Nearly Incompressible Transverse Isotropic (NITI) model.

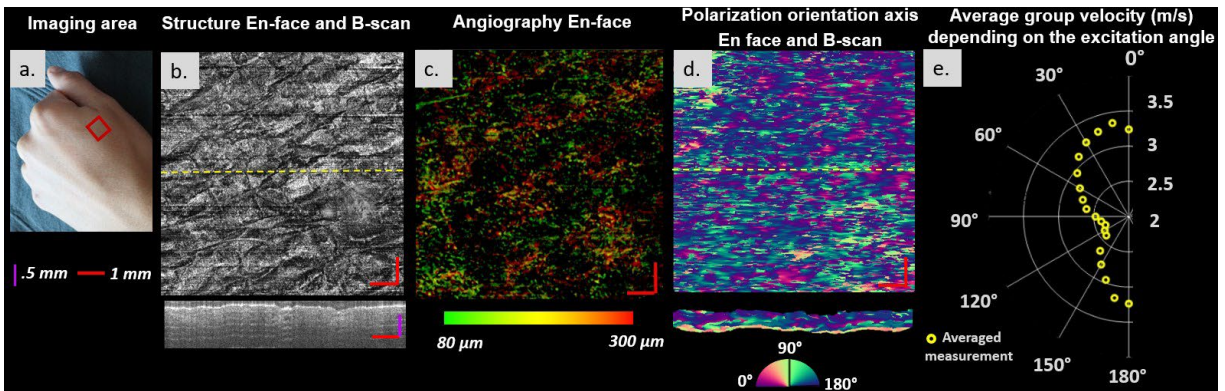


Figure 1. Photo of a scanned area (a.) with the resulting en-face and B-scan structure (b.), angiography projection (c.), polarization orientation axis (d.) and OCE-measured Rayleigh-wave anisotropy (e.)

Results/Discussion

In-vivo measurements were performed on 12 healthy volunteers across three different skin sites: the palm, forearm, and dorsal side of the hand. Key differences between skin sites in tensile anisotropy, epidermal thickness, and capillary density as well as cross-individual variability were observed.

Conclusion

The results demonstrate the system's capability and provide a foundation for future clinical studies aimed at evaluating skin graft surgeries.

Reconstructing Anisotropic Mechanical Moduli in Skin from Noncontact Dynamic Optical Coherence Elastography

Shyamal Guchhait¹, Agathe Marmin¹, Raveeroj Bawornkitchaikul¹, Clayton Ellington¹, Tam Pham², Russell Ettinger², Ruikang K. Wang¹, Matthew O'Donnell¹ and Ivan (Vanya) Pelivanov¹

¹Department of Bioengineering, University of Washington, Seattle, USA

²Harborview Medical Center, University of Washington, Seattle, USA

Background, Motivation, and Objective

Precise non-invasive elasticity measurement in skin is vital for reconstructive surgery, burn care, and scar management. This study describes a method of local reconstruction of anisotropic mechanical properties in skin from non-contact dynamic Optical Coherence Elastography (OCE).

Statement of Contribution/Methods

Collagen fibers in dermis drive skin's elasticity. Here we use Rayleigh wave speed angular anisotropy to locally reconstruct all 3 mechanical moduli with nearly incompressible transverse isotropic (NITI) model.

Result/Discussion

Figure 1 represents a typical situation of the OCE scanning. A plane Rayleigh wave launched by an air-coupled cylindrical transducer propagates over the skin surface (b) covering about a 9 mm x 9 mm area (c). The propagation is repeated for 19 propagation directions with a step of 10 degrees. Combining all propagation directions together (d) allows to compute the Rayleigh wave speed anisotropy in every point of the scanning area and finally perform fitting with the NITI model to reconstruct the moduli.

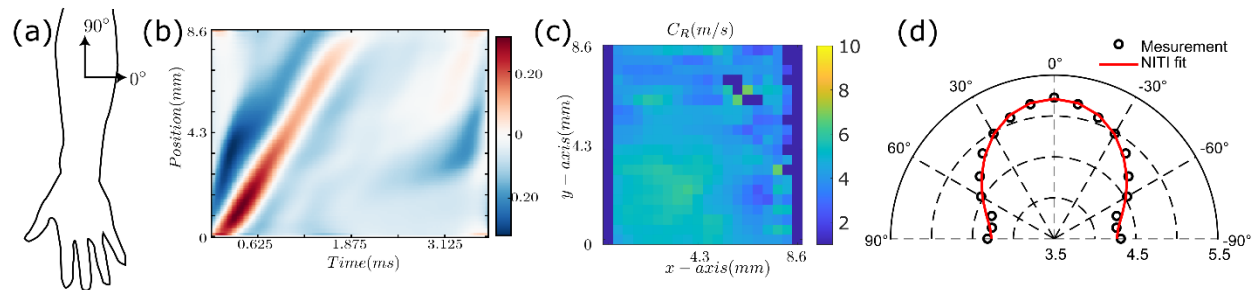


Figure 1. Typical anisotropy of Rayleigh wave propagation in a forearm region of a healthy volunteer: (a) diagram of measurement, (b) distance-time plot, (c) spatially resolved wave speed in one of the propagation directions, (d) measured anisotropy of Rayleigh wave speed with an interleaved NITI fit.

Conclusions

This study demonstrates that all 3 mechanical moduli in skin can be locally reconstructed using Rayleigh wave speed anisotropy measured with non-contact dynamic OCE. The established routine is used now in assessment of skin's moduli in a population of normal subjects and will then be used in scanning skin graft surgery patients.

Study and Reconstruction of the Mechanical Endometrial Tumor Microenvironment Using Microelastography

Malaury Devissi¹, Sibylle Grégoire¹, Charlotte Rivière², Axelle Brulport¹, Stefan Catheline¹

¹ Université Claude Bernard Lyon 1, Centre Léon Bérard, INSERM, LabTAU, LYON, France

² Institut Lumière Matière (ILM), Université Claude Bernard, Villeurbanne, France

Background, Motivation and Objective

Endometrial cancer was considered in 2022 as the 6th most common female cancer with more than 420,000 new cases this year. A proportion of aggressive stages is therapy-resistant and lethal for women with an overall survival at 5 years of less than 50% compared to early stages (stage I, 90%). This finding highlights the lack of therapeutic solutions for the treatment of this cancer. The objective of this project is to build a platform to study therapy response of endometrial cancer by reconstituting the tumor's cellular and mechanical environment. To reconstruct the mechanical environment of endometrial cancer, the elasticity of tumors and tumoroids derived from them was studied by microelastography.

Statement of Contribution/Methods

In this study, microelastography was used to recover mechanical properties in tumoroids. Thanks to a piezoelectric transducer, a frequency sweep (100 Hz – 15 kHz) was sent to agarose embedded tumoroids, and a video of propagating waves was recorded with an ultrafast camera at 30,000 fps. These videos were treated with a correlation algorithm which permitted calculation of the shear wave speed and estimation of the Young's modulus in the objects under study.

Results/Discussion

Experiments show that the algorithm can detect shear waves in a little object, such as a tumoroid of about a 100 μm in size, and enables the estimation of the shear wave speed (~ 0.65 m/s) and the Young's modulus of the tumoroids (~ 1.3 kPa), giving crucial information on the tumor micro-environment.

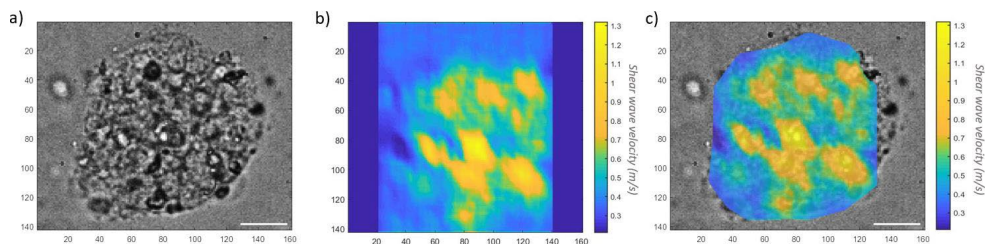


Figure 1. Tumoroid shear wave velocity estimation by microelastography. a) Brightfield image of the tumoroid (scale bar: 100 μm). b) Shear waves velocity map. c) Merge of the two images (scale: 100 μm).

Conclusions

We have shown that we were able to recover shear waves velocity and make an estimation of the Young's modulus of tumoroids, which will enable us to recreate the tumor microenvironment in a dedicated agarose-based platform. We will investigate whether tumor stiffness can be used as a predictive marker of its resistance to treatment.

Gravitational Lense Effect in a Soft Fabric Membrane

*Stefan Catheline*¹, *Victor Delattre*¹, *Gabrielle Laloy-Borgna*¹, *Frédéric Faure*² and *Mathias Fink*³

¹ LabTAU, INSERM, Centre Léon Bérard, Université Claude Bernard Lyon 1, Lyon, France

² Institut Fourier, Université de Grenoble, Grenoble, France

³ Institut Langevin ESPCI, Université de Paris, Paris, France

Background, Motivation and Objective

This work is devoted to elastic waves on soft membranes. More precisely, although optical elastography is used, the motivation of this work is not medical but rather physical: we aim at studying topological effects on soft membrane waves. Soft elastic membranes are often used as didactic demonstration of gravitation from the general relativity perspective. Indeed, trajectories of rolling spheres such as billiard balls influence each other through the deformation their mass print within the membrane tissue as would the space-time curvature of gravity. The analogy is pushed here using soft membrane waves. This allows revisiting through membrane waves, the famous 1919 Eddington experiment that demonstrated light deviations of stars in the vicinity of the sun.

Statement of Contribution/Methods

The experiment was conducted with a fabric membrane stretched over a 25 cm diameter drum pad (Figure). Different fabrics were tested: swimsuit, pantyhose (tights), and sweater (pullover). The sweater fabric was 100% cotton, and a 2-cm grid aligned with the fiber orientation was drawn on it. Waves were launched using a wooden ruler which was carefully positioned along the main direction of the fibers to avoid undesirable nonisotropic effects of propagation across the fabric membrane.

Results/Discussion

We show that wave propagation past a topological deviation on a two-dimensional flat fabric membrane is analogous to gravitational lensing. Using an ultrafast camera, we track a membrane plane wave as it crosses a local warped depression. Finite difference simulation, based on the scalar wave equation in a Schwarzschild metric, fully describes the experimental wavefront shape. Comparison between the theoretical and experimental deviation of wave geodesics from straight lines shows that (i) the nonlinear behavior of fabrics due to stretching induces second order effects only and (ii) the experimental depression is closely approximated by the Schwarzschild metric of a gravity well. The experiment demonstrates, in a simple way, how wave propagation is influenced by the topology of the medium.

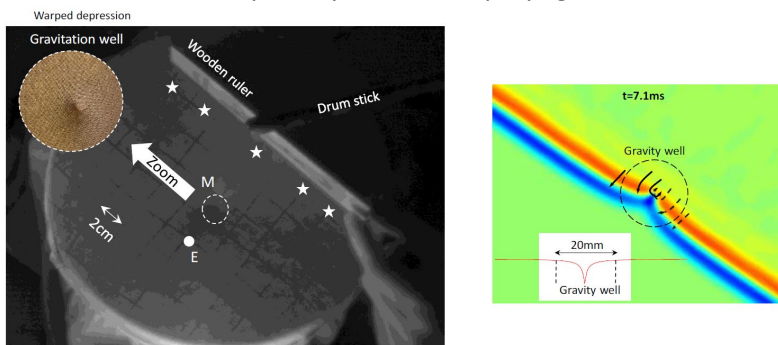


Figure 1. Membrane wave replica of Eddington's 1919 experiment. The topological deviation predicted for light near the sun is applied to a deformed membrane.

Abstracts



Friday, June 27th

Unveiling Tissue Secret Using Vibrations

Stefan Catheline

LabTAU, INSERM, Centre Léon Bérard, Université Claude Bernard Lyon 1, Lyon, France

The first part is devoted to human soft tissues. Elastography, sometimes referred to as seismology of the human body, is an imaging modality now implemented on medical ultrasound systems, on MRI and recently in optical coherence tomography devices. It allows to measure shear wave speeds within soft tissues and gives a tomography reconstruction of the shear elasticity. The shear elasticity being the elasticity felt by fingers during palpation, elastography is thus a palpation tomography. In the first part of this presentation, a passive elastography method is described. Inspired by noise correlation seismology and time reversal, it allows to extract from natural shear waves produced in the human body by heart beatings, muscles activities, arterial pulsations, a shear wave speed estimation. Therefore, an elasticity palpation mapping with no shear wave source is conducted. The latest developments in micro-elastography of a single cell will be described.

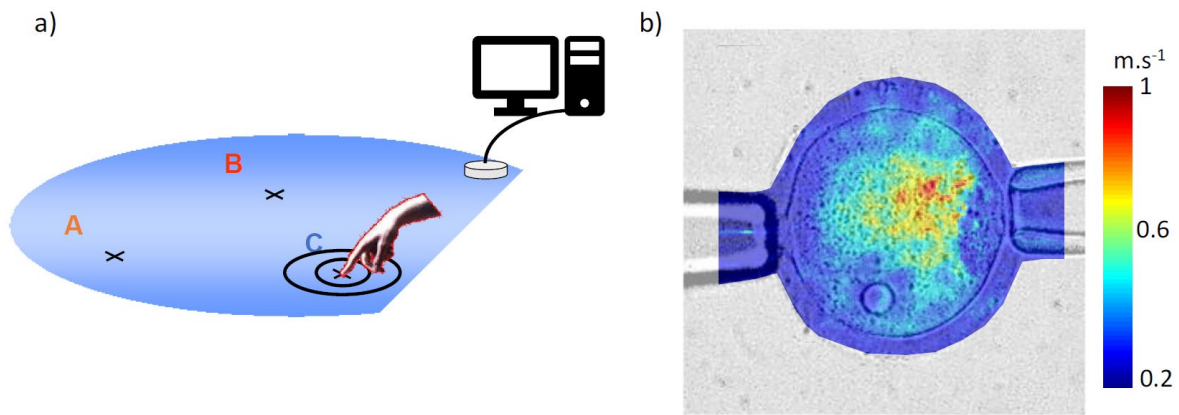


Figure 1. a) Experimental measurement of elasticity table, b) elasticity palpation of a single cell (oocyte).

Elasticity Mapping with High Intensity Focused Ultrasound for Prostate Ablation Treatment Planning

Tatiana Khokhlova^{1,2}, Gerald Lee^{2,3}, Oleg Sapozhnikov², Pavel Rosnitskiy¹, George Schade⁴

¹ University of Washington School of Medicine, Division of Gastroenterology, Seattle, WA, USA

² Applied Physics Laboratory, Center for Industrial and Medical Ultrasound, Seattle, WA, USA

³ University of Washington, Department of Bioengineering, Seattle, WA, USA

⁴ University of Washington School of Medicine, Department of Urology, Seattle, WA, USA

Background, Motivation and Objective

The efficacy of Prostate Cancer (PCa) ablation with endorectal high-intensity focused ultrasound (HIFU) depends on defining accurate tumor margins during treatment planning. US imaging fusion with pre-operative MRI currently used for this purpose frequently underestimates the tumor size. Shear wave elastography (SWE) is a promising method to outline stiff PCa tumors, but has depth limitations and lacks built-in arrangements with clinical HIFU systems. The objective here was to develop and validate a HIFU-push method of SWE that would overcome the limitations in the context of PCa ablation.

Statement of Contribution/Methods

A 128-element 1.6 MHz endorectal HIFU array driven by Verasonics system was used for emission of a 500-microsecond push, and the tracking pulses from a coaxial US imaging probe measured the tissue displacement resulting from propagation of longitudinal SW (LSW) along the HIFU axis. Both the push and the tracking beam were steered within the US imaging plane to obtain a 2D elasticity map. The method was tested in homogenous tissue-mimicking gels (6%, 8.75%, and 10% polyvinyl alcohol, 6% Al₂O₃ powder) with elastic moduli calibrated by a clinical SWE imaging system (SSI Aixplorer), in commercial SWE phantom, and in human prostatectomy tissue with tumor margins subsequently identified histologically.

Results/Discussion

The group velocity of LSW propagation along the HIFU axis, both towards and away from the transducer, was observed to be higher than SW velocity by a constant factor dependent on the HIFU field shape. The mean elastic moduli of the homogenous phantoms with increasing PVA concentration measured by HIFU-LSWE method yielded the values of 8, 29 and 83 kPa. This range is representative of benign and cancerous prostatic tissue and closely corresponded to measurements with SSI - 9, 29 and 66 kPa, respectively. 2D HIFU-LSWE allowed to visualize stiff inclusions in commercial SWE phantom, and the elasticity measurements in prostatectomy specimens aligned with the expected elastic modulus range of 20-80 kPa.

Conclusions

HIFU-LSWE is a promising quantitative method of mapping target tissue elasticity and can be used for both planning and assessing the outcomes of ablative HIFU treatments of the prostate and other tissues.

Diaphragm Loading Induced Changes in Shear Modulus as Assessed with Ultrasound Shear Wave Elastography in Absence of Detectable Contractile Fatigue

Axel Nierding^{1,2}, Eloïse Chamalet^{1,3}, Corentin Cornu², Damien Bachasson^{1,3}, Jean-Luc Gennisson².

¹Sorbonne Université, INSERM, Neurophysiologie Respiratoire Expérimentale et Clinique, Paris, France

² Université Paris-Saclay, Inserm, CNRS, CEA, BioMaps, Orsay, France

³ Institute of Myology, Neuromuscular Investigation Center, Paris, France

Background, Motivation and Objective

Changes in the shear modulus (μ) were shown to be associated with muscle fatigue and structural damage. The study aimed to (1) investigate if resting modulus (μ_{di}) is altered after inspiratory loading task, and (2) examine the relationship between changes in μ_{di} and contractile diaphragm fatigue, assessed with transdiaphragmatic twitch pressure (Pdi_{tw}) measurement elicited by cervical magnetic stimulation.

Methods

Eleven healthy volunteers were studied. Diaphragm SWE was performed at the right costal hemidiaphragm's zone of apposition using an Aixplorer (Supersonic Imagine, France) driving an SL10-2 linear array. Ten-second SWE acquisitions were performed during an apnea at functional residual capacity. Cervical magnetic stimulation was performed by using a Magstim 200 stimulator (Magstim, UK) (Fig.1a).

Results/Discussion

A significant decrease in μ_{di} was observed following inspiratory loading (12.4 ± 4.23 kPa versus 9.70 ± 3.00 kPa, $p < 0.05$ (Fig. C). No significant difference was observed in Pdi_{tw} following inspiratory loading, and no significant correlation between changes in μ_{di} and Pdi_{tw} was found ($r = -0.24$, $p = 0.29$).

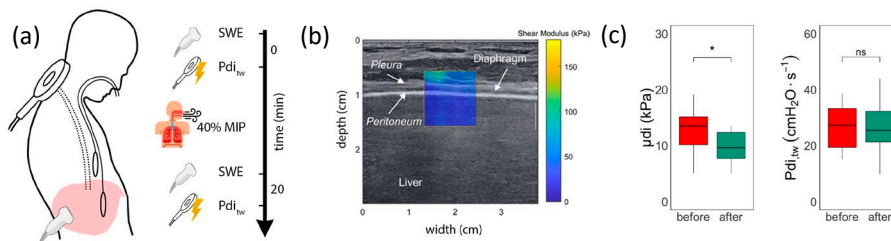


Figure 1. a) Diaphragm modulus (μ_{di}) assessed with SWE and twitch transdiaphragmatic pressure (Pdi_{tw}) were measured before and after a 20 min inspiratory loading at 40% of max inspiratory pressure. b) An image obtained during diaphragm SWE. c) μ_{di} and Pdi_{tw} before and after inspiratory loading.

Conclusions

These preliminary findings indicate that inspiratory loading induced significant change in diaphragm mechanical properties even in absence of a measurable drop in Pdi_{tw} . By enabling noninvasive, real-time monitoring of μ_{di} , SWE may offer a clinically feasible means to assess early changes in diaphragm mechanics. Further investigations in critically ill populations could elucidate how ventilatory strategies might be optimized to preserve diaphragm function and improve weaning outcomes.

Pulse Wave Imaging for Early-Stage Atherosclerosis Monitoring and Detection: a Preliminary Study in Hypercholesterolemic Swine Model

*Haokang Shi*¹, *Pengcheng Liang*¹, *Parth Gami*¹, *Tuhin Roy*¹, *Rosalía Minyety*¹, and *Elisa E. Konofagou*¹

¹Columbia University, New York, USA

Background, Motivation and Objective

Early-stage atherosclerosis can be characterized by the localized presence of endothelial dysfunction, accompanied by inflammation and fibrosis. Pulse wave imaging (PWI) is a non-invasive, ultrasound-based elasticity technique that can be utilized to estimate the mechanical properties of arterial walls, including plaques. This study utilized PWI in a hypercholesterolemic swine model to assess its potential for early-stage atherosclerosis detection and monitoring.

Statement of Contribution/Methods

Three (n = 3) male Wisconsin Mini Swine-Familial Hypercholesterolemic (WMS-FHTM) were acquired from the University of Wisconsin Swine Research Farm and fed an atherogenic diet (15% lard, 1.2% cholesterol). To initiate endothelial cell injury and early-stage atherosclerosis development, a procedure to induce balloon catheter injury was conducted on the right carotid of each swine, while the left carotid remained intact. Both carotid arteries were longitudinally monitored post-operatively over three months with PWI. For arterial wall motion estimation, a 1D normalized cross-correlation technique was applied on the compounded RF frames, resulting in a frame rate of 2667 kHz. The pulse wave velocity (PWV) at end-diastole was estimated using linear regression based on the spatiotemporal map of axial wall distention acceleration, representing the second derivative of the wall displacement. The Bramwell-Hill equation was used to estimate and image the compliance of the carotid wall.

Results/Discussion

The temporal PWV changes of the injured common carotid depicted that PWV increased by over 100% immediately after surgery (Day 0) and returned to baseline within 10 days, while compliance dropped by 85% and recovered to baseline. For the intact carotid, it was observed that PWV gradually increased over the next three months, reaching a 44% elevation, while compliance decreased by 37% on average. A balloon catheter injury can cause endothelial remodeling, and endothelial cells are susceptible to injury but replicate quickly, which could explain the PWV and compliance changes within the first 10 days post-injury. In the intact carotid, the sustained simultaneous increase in PWV and decrease in compliance may also reflect the effects of the atherogenic diet. A significantly larger PWV ($p < 0.05$) and significantly lower compliance ($p < 0.05$) were observed in the injured carotid of Swine #3. Although no significant difference was found in PWV or compliance between the injured and intact carotid in Swine #1 and Swine #2, similar trends were obtained. The differences in results among swine may be due to individual variability in response to the atherogenic diet and differences in the degree of surgical injury.

Conclusions

In conclusion, this preliminary study highlights the potential of PWI for monitoring of endothelial, providing an early detection approach for early-stage atherosclerosis onset.

Ultrasound Time-Harmonic Elastography for the Assessment of Induced Muscle Stiffness in Response of Tonic Vibration Reflex

Hossein S. Aghamiry¹, Tom Meyer¹, Stefan Klemmer Chandia¹, Yanglei Wu¹, Ingolf Sack¹

¹ Department of Radiology, Charité – Universitätsmedizin Berlin, Berlin, Germany.

Background, Motivation and Objective

Tonic Vibration Reflex (TVR) is a neuromuscular response characterized by involuntary muscle contractions due to sustained mechanical vibration. It enhances proprioception, motor control, and muscle tone, with potential applications in neuromuscular rehabilitation. This study investigates the impact of TVR on vastus lateralis (VL) muscle stiffness in healthy volunteers using ultrasound time-harmonic elastography (THE).

Statement of Contribution/Methods

A controlled 100 Hz vibration was applied to the VL tendon (Fig. 1a) to modulate muscle tone via TVR. Shear wave speed (SWS), a proxy for muscle stiffness, was measured before and during TVR stimulation using a multifrequency vibration source (60, 70, and 80 Hz) and a standard ultrasound scanner (GAMPT GmbH) with frame rate precisely matching the TVR frequency. The k-MDEV method was employed for data analysis and extracting SWS maps. 11 healthy volunteers (39 ± 16 years) participated in this study.

Results/Discussion

TVR significantly increased muscle stiffness as can be seen in Fig. 1b for one of the volunteers over time and Fig 1c for mean values of all the volunteers. Mean SWS rose from 1.72 ± 0.10 m/s (baseline) to 1.94 ± 0.16 m/s with medium-amplitude stimulation ($p < 0.0001$, $d = 2.24$) and 2.03 ± 0.17 m/s with high-amplitude stimulation ($p < 0.00001$, $d = 3.01$). Paired t-tests confirmed significant stiffness increases under both stimulation conditions, with higher amplitudes producing stronger effects.

Conclusions

We showed that TVR effectively modulates muscle stiffness, underscoring its potential as a marker for muscle function in THE and a therapeutic tool in rehabilitation medicine. THE offers a robust approach for capturing dynamic changes in muscle properties, providing insights into neuromuscular function.

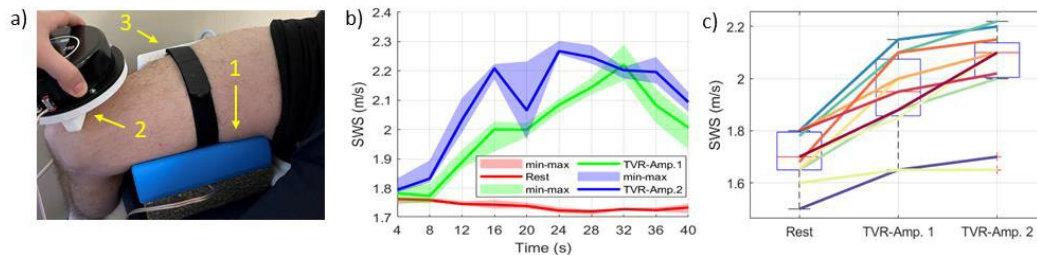


Figure 1. (a) Experimental setup: a THE source beneath the thigh (1), and an actuator (2) applies vibration to the tendon for TVR. An ultrasound probe (3) is secured with a belt for stability. (b) SWS over time for a volunteer at rest (red) and under TVR stimulation at different amplitudes (green and blue). (c) Box plot summarizing SWS measurements for all volunteers (shown with color-coded lines).

Abstracts



Saturday, June 28th

Multi-Frequency Time Harmonic Elastography Across Scales, Dynamics, and Platforms

Ingolf Sack

Department of Radiology, Charité – Universitätsmedizin Berlin, Berlin, Germany.

The viscoelastic behavior of soft biological tissues results from the hierarchy of biomechanical interactions among cells, matrix, and fluid compartments. Consequently, mapping viscoelastic parameters by in vivo elastography opens a door to the emergent behavior of tissue constituents at a much smaller length scale than provided by coarse-grained image resolution. However, the complexity of biomechanical interactions requires consideration of the dynamic range and mode of mechanical stimulation. Time harmonic elastography uses shear waves of precisely known frequency to interrogate the viscoelastic response of body tissues such as brain, heart, or liver; micro-systems such as single cells, biofilms, or zebrafish; or biological material models such as glycosaminoglycans, polymer solutions, or decellularized tissues. Wave encoding can be achieved by MRI, ultrasound or optical lenses, while uniform inversion schemes ensure comparable values despite this wide variety of systems, platforms and length scales. This talk will provide an overview of the various measurement principles of time harmonic elastography with a focus on the use of multifrequency shear waves for high-resolution biomechanical mapping or analysis of viscoelasticity

Combined MR Elastography and 3D MRI Deformation Mapping Towards *in vivo* Assessment of Solid Stress in Glioblastoma

Noah Jaitner¹, Mehrgan Shahryari¹, Jakob Schattenfroh¹, Jakob Ludwig¹, Tom Meyer¹, Ingolf Sack¹

¹ Department of Radiology, Charité-Universitätsmedizin, 10117 Berlin, Germany

Background, Motivation and Objective

Glioblastoma, an aggressive brain tumor, disrupts the structure of the surrounding tissue and alters its biomechanical properties by exerting mechanical stress. While altered stiffness properties due to tumor progression can be measured by MR elastography (MRE) *in vivo*, solid stress assessment additionally requires 3D deformation analysis. Therefore, we combined MRE and 3D MRI deformation mapping in a group of patients with glioblastoma to quantify tumor-stress associated stiffening of brain tissue.

Statement of Contribution/Methods

Seventeen patients (4 women, 50 ± 13 years) with glioblastoma and twelve healthy volunteers (3 women, 33 ± 9 years) were studied with MRE (20, 25, 30 and 40 Hz) and T1 imaging. Imaging examinations were performed in a 3T MRI scanner (Magnetom Lumina, Siemens, Erlangen, Germany) using a 32-channel head coil. Shear wave speed (SWS) maps were generated using k-MDEV. Displacement fields were determined by 3D image registration to the standard brain atlas using TransMorph.

Results/Discussion

Registration of 3D brain MRI to a standard brain atlas showed higher displacement magnitudes near tumors than in distant regions or in normal controls ($p < 0.001$). Brain stiffness correlated with displacement magnitude particularly in peritumoral regions where the displacement magnitude exceeded 90% of that of unaffected brain regions ($R = 0.51$, $p = 0.04$).

Conclusions

This study shows that combining MRE and 3D MRI deformation mapping is sensitive to solid-stress induced stiffening in brain regions near glioblastoma. The observed correlation of brain deformation with brain stiffness suggests hyperelastic stiffening caused by tumor expansion. Regions characterized by high deformation were heterogeneously distributed around the tumor core, suggesting the involvement of heterogeneous brain mechanical structures into tumor expansion patterns and disrupted normal brain anatomy.

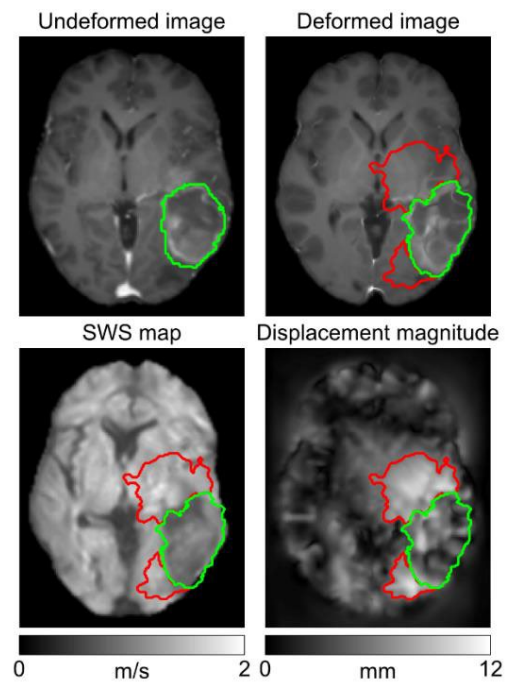


Figure 1. Undeformed image, deformed image, *SWS* map and deformation magnitude of a patient with glioblastoma. The glioblastoma is marked in green and areas of high displacement magnitude are in red.

Association of Gut Microbiome with MASLD and MASH and Its Correlation with MR Elastography in Mice

Biru Huang¹, Tom Meyer¹, Jakob Ludwig¹, Yasmine Safraoui¹, Noah Jaitner¹, Mehrgan Shahryari¹, Patrick Asbach¹, Ingolf Sack¹, Jing Guo¹

¹ Charité – Universitätsmedizin Berlin, Department of Radiology, Berlin, Germany

Background, Motivation and Objective

Gut microbiome, comprising bacteria, archaea, protists, fungi, and viruses is implicated in MASLD and MASH. However, its role in disease progression and its correlation with MRE parameters remains unclear. This study explores its contributions in MASLD/MASH and its correlation with MRE parameters.

Statement of Contribution/Methods

MASLD/MASH was induced in 44 male C57BL/6J mice using a high-fat, low amino acid diet. In vivo multi-frequency MRE was performed using a 3T MRI scanner at different timepoints providing shear wave speed (SWS) and penetration rate (PR) as proxies of stiffness and viscosity. Livers and fecal samples were collected post-mortem. DNA was extracted from fecal samples, and predominant bacterial groups were assessed by qRT-PCR using 16S rRNA gene primers.

Results/Discussion

Numbers of predominant bacterial groups showed significant changes over disease progression. Particularly the number of Mouse Intestinal Bacteria (MIB) significantly decreased with disease severity ($p < 0.001$, $R = -0.8$). Correlation analysis revealed significant associations between gut microbiome and PR, particularly for MIB ($p < 0.001$, $R = -0.42$), Eubacteriaceae (EubV3) ($p = 0.01$, $R = -0.4$), and Clostridium leptum (sgClep) ($p < 0.001$, $R = -0.53$), while correlation with SWS remained unchanged.

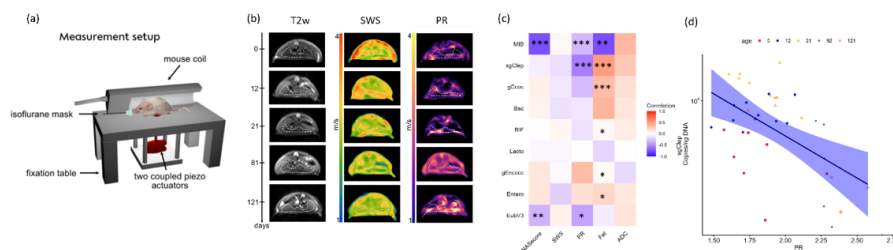


Figure 1. (a) measurement setup (b) T2w images, SWS maps and PR maps (c) correlation between gut microbiome and NAS score, SWS, PR, ADC and fat accumulation. (d) correlation of sgClep with PR.

Conclusions

Our results indicated that the gut microbiome underwent significant changes over MASLD/MASH progression in mice, likely linked to metabolic processes and inflammation. The observed correlations between gut microbiome and PR, suggest that MIB ($p = 3e-04$, $R = -0.82$), EubV3 ($p = 0.01$, $R = -0.46$), and sgClep ($p = 0.002$, $R = -0.43$) influence disease progression, possibly through hepatic inflammation and fibrosis. The observed sensitivity of viscosity-related PR could be leveraged as a non-invasive biomarker for early detection and monitoring of MASLD/MASH in humans.

An Elastographic Atlas of the Aging Mouse Brain

Biru Huang¹, Rafaela Vieira da Silva², Tom Meyer¹, Jakob Ludwig¹, Anna Morr¹, Noah Jaitner¹, Carmen Infante-Duarte², Ingolf Sack¹, Jing Guo¹

¹ Charité – Universitätsmedizin Berlin, 10117 Berlin, Germany

Background, Motivation and Objective

The viscoelastic properties of brain tissue serve as a biophysical marker of nervous system composition and organization. MR elastography (MRE) can quantify cerebral biomechanics *in vivo*, capturing structural changes in health and disease. However, the aging brain's biomechanics signature and microstructural correlation remain unclear. This study aims to systematically analyze regional cerebral biomechanics in elderly mice and generate an elastographic atlas of the aging mouse brain.

Statement of Contribution/Methods

In groups of 29 female C57BL/6J mice aged between 6 to 18 months, changes of shear wave speed (SWS) and penetration rate (PR) as proxies of stiffness and inverse attenuation, were investigated using multifrequency MRE. Total acquisition time for 7 coronal slices of 0.18×0.18×0.8 mm resolution was 9 mins. All MRE parameter maps were registered to the Allen mouse brain atlas via their corresponding anatomical T2w images. Regions of interest prescribed by the atlas were used for substructure analysis.

Results/Discussion

SWS atlases of the mouse brain reflected age-related global softening ($-6.9 \pm 1.3\%$, $p = 0.02$) and an increase in viscosity ($3.5 \pm 0.4\%$, $p = 0.004$). While viscosity of white matter and gray matter showed the same course of change, stiffness reduction was more pronounced in WM ($-7.0 \pm 1.0\%$, $p = 0.002$) than GM ($-7.3 \pm 1.4\%$, $p = 0.045$). A preliminary elastographic atlas of the aging mouse brain is shown in Fig. 1.

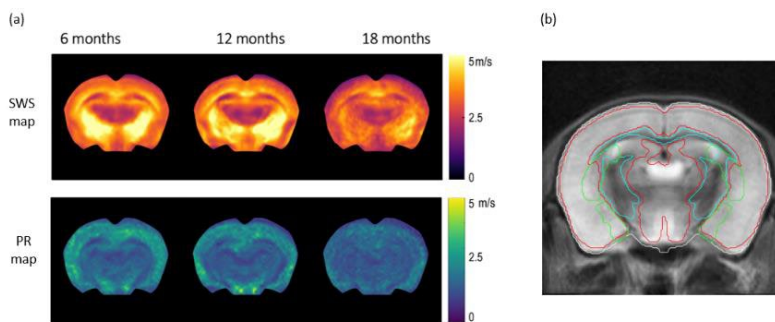


Figure 1: (a) Elastographic mouse brain atlas of SWS and PR averaged over 29 female mice at three age points. (b) ROIs of the whole brain (white), white matter (cyan), grey matter (red), and striatum (green) prescribed by the standard Allen brain atlas.

Conclusions

Our study provided the first elastographic atlas of the *in vivo* elderly mouse brain showing detailed anatomical structures over aging. The global brain softened with increased viscosity during aging, indicating a progressive degradation of brain tissue to a more fluid-like state with reduced rigidity. This observation complements previous findings of increasing solid-rigid structures in the maturing mouse brain.

Multi-plane Shear Wave Elastography: Towards 3D Imaging of Tissue Viscoelasticity

Ryan Pitsinger, Abdelrahman Elmeliegy, Murthy N. Guddati

NC State University, CCEE Computing and Systems, Raleigh, NC, United States

Background, Motivation and Objective

Elasticity imaging using shear wave elastography (SWE) is well-established, but the reconstruction of viscosity maps remains a challenge. Moreover, current imaging algorithms, even for elasticity, are limited to imaging within the measurement plan. Our ultimate goal is to develop imaging algorithms that provide fully 3D images, including in the elevational plane, of not only elasticity but also viscosity.

Statement of Contribution/Methods

We utilize full waveform inversion (FWI) where the misfit between measured and simulated measurements is minimized by iteratively adjusting the viscoelasticity map of the imaging domain, using adjoint-based gradient optimization approach. We bring together various ideas to ensure convergence of FWI, specifically informed by the underlying physics of the problem. These include (a) correlation-based objective, (b) multi-resolution inversion to progressively refine reconstructions (c) mitigating cross-talk between elasticity and viscosity through sequential inversion, and (d) multi-plane illumination.

Results/Discussion

We illustrate the effectiveness of our approach by tackling a lower dimensional model problem: computing 2D imaging from 1D measurements (as opposed to 3D imaging from 2D measurements). Figure 1 shows true images of elasticity and viscosity, as well as those obtained from our methodology (we specifically highlight the effect of multi-plane illumination by showing the difference between single plane excitation and three-plane excitation, but the benefits of other ideas listed above will be presented in the talk).

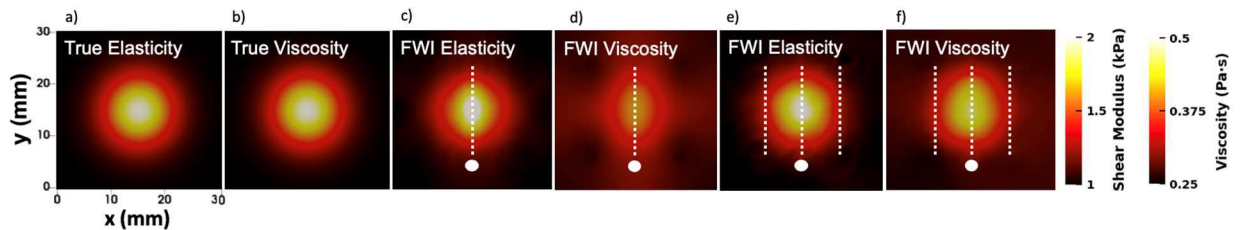


Figure 1. True (a, b) and FWI-reconstructed (c–f) elasticity and viscosity with 15 dB noise. Single-plane (c, d) vs. multi-plane (e, f) excitation. Color bars show shear modulus (kPa) and viscosity (Pa-s).

Conclusion

Our approach, after appropriate validation, could lead to MRE-type 3D images of elastic modulus and viscosity but from SWE using linear US arrays.

3-D Single Transducer-Harmonic Motion Imaging Using a Row-Column-Addressed (RCA) Array

Yanpei Liu¹, Shiqi Hu¹, Saachi Munot¹, and Elisa E. Konofagou¹

¹Columbia University, New York, NY, USA.

Background, Motivation and Objective

Harmonic motion imaging (HMI) is an ultrasound elasticity imaging technique that measures the viscoelastic properties of tissue by inducing oscillatory motion. The resulting dynamic displacements, inversely proportional to the local stiffness. This study introduces 3-D HMI using a handheld RCA array.

Statement of Contribution/Methods

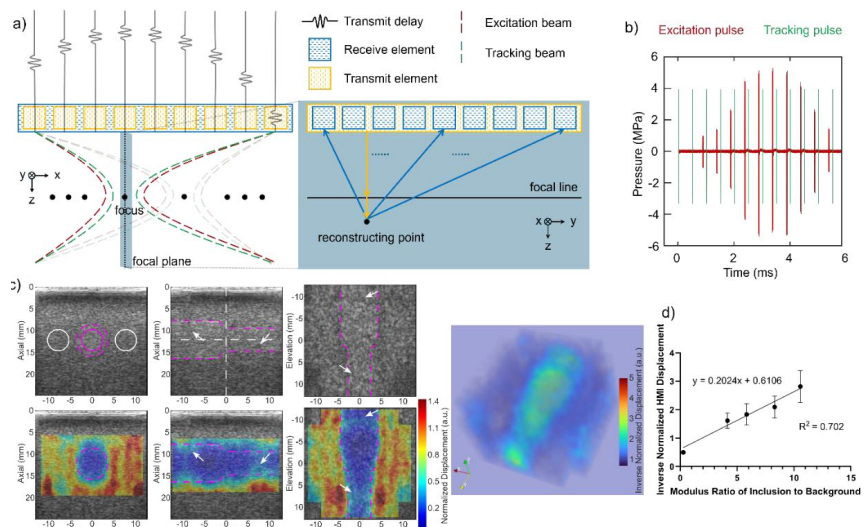
A commercially available RCA array (RC6gV, 6 MHz, 128 row and 128 column elements) was used (Fig. 1a). Row (column) elements driven at 4.2-MHz were used for excitation, and the same elements driven at 6.9-MHz were used for tracking with the perpendicular column (row) elements receiving. A 33-ms interleaved sequence (Fig. 1b) comprising 500- μ s pulses (2000 Hz) was used, which consisted of 30- μ s focused excitation (red) followed by 120- μ s idle time to reduce interference between excitation and tracking, and a 1.5-cycle focused tracking (green). The amplitude of excitation pulses was modulated at 200 Hz to induce oscillatory displacement. IRS elasticity phantoms with stepped-cylindrical inclusions of different diameters and Young's moduli were imaged.

Results/Discussion

The 3-D HMI data acquisition lasted 2 seconds using the RCA to cover a volume of 20x20x15 mm³. Representative tri-plane B-mode and HMI images are shown in Fig. 1c, along with 3-D HMI rendering of a 56-kPa stepped-cylindrical inclusion (diameters: 5.0 and 8.6 mm). 3D-HMI was able to detect the transition from large to small inclusions with a contrast of 0.34. A linear regression was fit between the inverse normalized HMI displacement and modulus ratio of the inclusion to background with an R² value of 0.702 (Fig. 1d).

Conclusions

3-D HMI was hereby demonstrated using an RCA to achieve robust and time-efficient volumetric mapping of relative stiffness. This increases the clinical potential of HMI to assess tumor heterogeneity in mechanical properties.



Four-Dimensional (4D) Ultrasound Shear Wave Elastography Using Sequential Excitation

*Xin Sun*¹, *Chi-Feng Chang*¹, *Junhang Zhang*¹, *Yushun Zeng*¹, *Bitong Li*¹, *Yizhe Sun*¹, *Haochen Kang*¹,
*Hsiao-Chuan Liu*¹, *Qifa Zhou*¹

¹ Department of Biomedical Engineering, University of Southern California, USA

Background, Motivation and Objective

To explore mechanical properties of biological tissues in 3D, a 4D (x, y, z, t) ultrasound shear wave elastography is required. However, it is still challenging due to the limitation of the hardware of standard ultrasound acquisition systems. In this study, we introduce a novel method to achieve 4D shear wave elastography, named sequential-based excitation shear wave elastography (SE-SWE).

Statement of Contribution/Methods

A schematic diagram of experiment system setup is shown in Fig. 1(a). An ultrasound scanner (Vantage 256, Verasonics, USA) and an 8 MHz 1024-element 2D matrix array (Matrix1024-8, Verasonics) were used for data acquisition. For the excitation, a sinusoidal to generate the excitation.

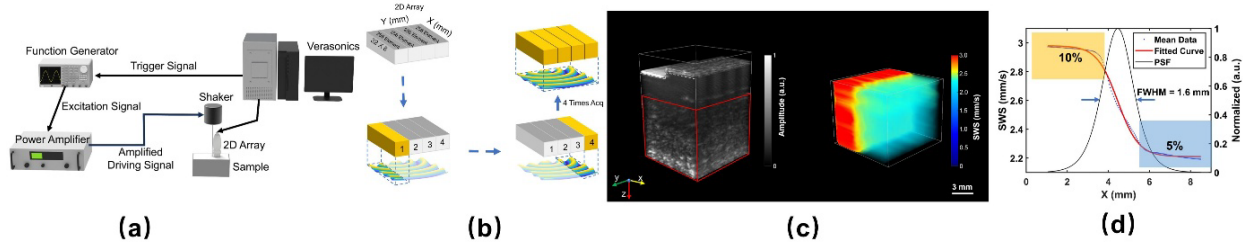


Figure 1. (a) Experimental setup of the external vibration-based 3D SWE sample study. (b) Volumetric image of the shear wave propagation. (c) 3D image and SWS map, derived from the red-boxed region. (d) SWS shift curve. The scatter plot represents the mean shear wave speed shift across the volume.

Results/Discussion

As Fig. 1 shows, the B-mode image exhibits minimal contrast for the 3D information. From the contours observed, the section on the left, which is shorter, is composed of 10% gelatin, whereas the right side consists of 5% gelatin. Fig. 1(c) shows the 3D SWS image, which shows a highly correlated morphological structure. The field of view was designated as an area within the red box in Fig. 1(c). Fig. 1(d) shows the FWHM resolution results (1.6 mm in x-direction), calculated from the fitted sigmoid function.

Conclusions

In conclusion, our Phantom studies validate the SE-SWE method as a highly accurate, reliable, and efficient technique for 3D shear wave elastography. Its success in these controlled experiments lays a solid foundation for the future in vivo applications, where its potential to improve the diagnosis and monitoring of various pathological conditions can be fully realized.

A Multigrid Scheme for Efficient Inversion Using a Finite-Volume Method

Joaquín Mura¹, Bruno Peña¹, Alfonso Caiazzo²

¹ Federico Santa Maria Technical University, Department of Mechanical Engineering, Santiago, Chile.

² Weierstrass Institute for Applied Analysis and Stochastics, Numerical Mathematics and Scientific Computing, Berlin, Germany.

Background, Motivation and Objective

Ultrasound elastography has demonstrated substantial clinical benefits across various conditions and is a promising imaging technique. However, the computational time required for inversion remains a significant hurdle, impeding its integration into clinical practice. In this study, we propose a method that combines a direct linear formulation for the complex shear modulus and utilizes a finite-volume approach. The inversion process is structured as an optimization problem, resolved using a multigrid scheme.

Statement of Contribution/Methods

Our study introduces a multigrid finite-volume method for efficiently calculating the complex shear modulus. We propose a direct inversion formulation based on a viscoelasticity model. Notably, this approach stabilizes the data assimilation process, allowing us to determine the shear modulus from time-harmonic tissue displacements accurately.

Results/Discussion

We tested a simulation of the incompressible viscoelastic wave using a fractional Zener model performed with FreeFem++ in a 2D unstructured mesh, composed by 59.262 nodes and 118.522 elements using Lagrange complex-valued finite element formulation. The parameters and configuration are displayed in Figs. 1a), b). The displacement data in Fig. 3c) was interpolated in a rectangular grid.

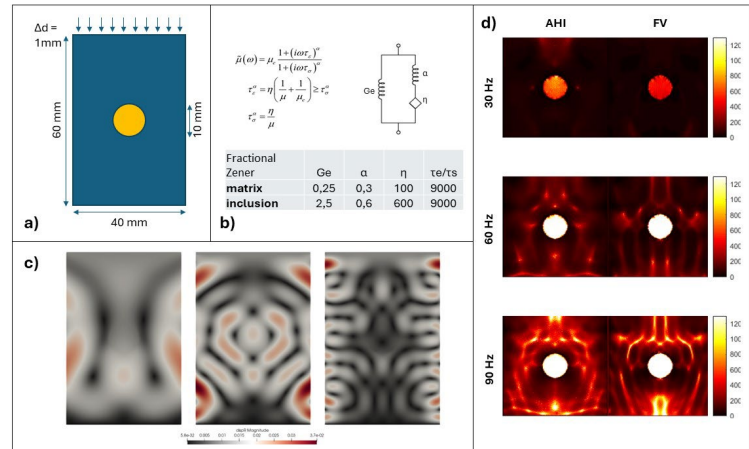


Figure 1. Comparison between FV and AHI (Algebraic Helmholtz Inversion) methods: (a) Geometric description of simulated phantom, (b) Parameters for Fractional-Zener tissue model, (c) Three snapshots of simulated waves, from left to right, at 30Hz, 60Hz, and 90Hz, (d) Inversion using AHI (first column) and FV (second column)

Conclusions

We present a novel scheme combining direct inversion for elastography and efficient multigrid optimization. This scheme appears to alleviate undesirable oscillations and instabilities in recovering the shear modulus found with other methods without sacrificing computational time.

Mechanical Characterization of Transverse Isotropy in Neuromuscular Tissues

Ricardo Andrade

Nantes Université, Nantes, France

Ultrasound shear wave elastography (SWE) has transitioned into routine clinical practice and is now widely applied for the detection and diagnosis of liver disease, cancer, and various other pathological conditions. By enabling the quantitative assessment of tissue mechanical properties, SWE has significantly expanded the diagnostic capabilities of ultrasound imaging. This presentation will emphasize the emerging application of conventional SWE for evaluating the mechanical properties of skeletal muscle and peripheral nerve tissues. Particular focus will be placed on SWE's ability to reveal new in vivo insights into the mechanical behavior of neuromuscular tissues, its potential clinical applications, and the challenges of accurately assessing these complex structures. The transversely isotropic nature of skeletal muscle and peripheral nerves will be discussed in terms of its impact on conventional SWE imaging, measurement accuracy, and clinical interpretation. Recent advances in angle-resolved elastography techniques will also be presented, with emphasis on their ability to estimate direction-dependent shear and tensile moduli, addressing key limitations of conventional SWE in characterizing transversely isotropic soft tissues. The potential of these emerging techniques to inform both disease state and biological response to therapy will be illustrated, underscoring their promise as noninvasive biomarkers in translational neuromuscular research and clinical practice.

Optimizing Multi-Modality Anisotropic Elasticity Imaging Phantoms

Kaden Bock¹, Shruthi Srinivasan¹, Kevin Eckstein², Samyuktha Kolluru², Juan Manuel Urueña³, Ned Rouze¹, Wren Wightman¹, Philip Bayly², Kathryn Nightingale¹

¹ Duke University, Biomedical Engineering, Durham, NC, United States

² Washington University, Mechanical Engineering & Materials Science, St. Louis, MO, United States,

³ University of California, NSF BioPACIFIC MIP, Santa Barbara, CA, United States

Background, Motivation and Objective

We present optimizations on the materials used to construct anisotropic lattice phantoms to better match the mechanical and acoustic properties of anisotropic tissues such as skeletal muscle [1].

Statement of Contribution/Methods

Isotropic phantoms were created from polyacrylamide (PAA). Anisotropic phantoms were made by embedding scaled lattice structures, made from either urethane methacrylate (UMA) or polyethylene glycol diacrylate (PEGDA), into the PAA background [4]. Lattice phantoms were characterized using 3D-Rotational SWEI (3D-RSWEI), in which multiple 2D SWEI acquisitions are gathered at 5° rotational spacing.

Results/Discussion

Isotropic PAA phantoms had SWS of 0.99 ± 0.10 m/s. PAA phantom SWS remained consistent to $\pm 4.9\%$ over 2 months. Lattice phantoms were characterized to have SWS of 4.6 ± 0.2 and 2.5 ± 0.1 m/s along and across the scaling direction of the lattice after embedding.

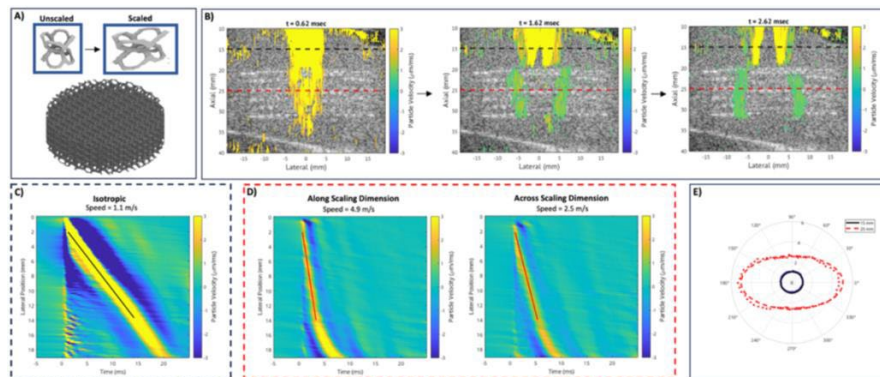


Figure 1. A) A 3D view of a scaled lattice. B) Visualization of shear wave propagation at 3 timepoints C) Above the scaled lattice (15 mm), shear waves propagate at the same speed at all rotational angles. D) Within the lattice (20mm) shear waves propagate faster and speeds vary for different rotational angles. E) Shear wave speed estimates at each rotational angle are fit to an ellipse to estimate SWS along and across the scaling direction.

Conclusions

We have been able to optimize anisotropic elasticity phantoms to mimic tissues of interest.

On The Stability of Time-Of-Flight-based Shear Wave Speed Estimators using Slowness and Velocity

Wren E. Wightman, Ned C. Rouze, Mark L. Palmeri, and Kathryn R. Nightingale

Duke University, Department of Biomedical Engineering, Durham, NC, USA

Background, Motivation and Objective

The measurement of shear wave speed (SWS) is essential in the quantification of elastic properties of soft tissue. The SWS c is often calculated so that $c = \delta x / \Delta T$, where δx is the distance and ΔT is the time-of-flight (TOF) between two observation points. Alternatively, the shear wave propagation rate can also be described by its slowness s , defined as the reciprocal of c , so that $s = \Delta T / \delta x$. In this study, we aim to demonstrate and compare the stability of SWS estimation using point estimates of c and s , quantified with both Monte Carlo simulations and evaluation of the trends in experimental data.

Statement of Contribution/Methods

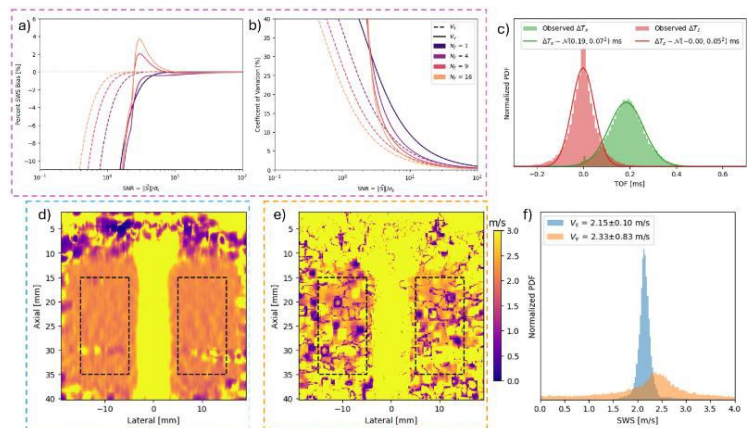
Monte Carlo simulations of velocity-based SWS V_v and slowness-based SWS V_s were drawn from TOF distributions corresponding to a 2D laterally propagating shear wave with a SWS of 2 m/s and $\delta x = 2$ mm. SWS reconstruction was evaluated across a range of TOF noise σ_T . Experimental data was acquired using a Verasonics Vantage system with a Phillips L7-4 probe in a 15.92 kPa (2.30 m/s) elasticity phantom. Experimental estimates of V_v were calculated with $\delta x = 0.4$ mm and window size of 2 mm axially. The estimates of V_s were computed from the inverse magnitude of the weighted average of s along each axis.

Results/Discussion

The simulated SWS bias and coefficients of variation (CoV) are shown in Figures (a) and (b) respectively. The bias magnitude and CoV of V_s were always lower than those of V_v . Figure (c) shows that experimental TOF is approximately normal in both the lateral and axial directions. The estimated SWS maps of V_s and V_v are shown in Figure (d) and (e) respectively. The variability of the SWS was much higher in the map of V_v than V_s . The distributions of V_s and V_v in Figure (f) were drawn from within the black dashed boxes in Figures (d) and (e). Notice that both the mode and mean of V were higher than V_s and the standard deviation of V_v was also higher than V_s .

Conclusions

In this case study, we demonstrated that slowness-based SWS had lower bias and variability across a range of SNRs. We conclude that slowness-based TOF SWS estimation is superior to velocity-based SWS estimation.



Elastography In Prestressed and Transversely Isotropic Viscoelastic Structures: Inverse Modeling Challenges

Alexandra Vorobyeva¹, Dieter Klatt¹, Ken Shull², Eric Perreault², Thomas J. Royston¹

¹ University of Illinois Chicago, Chicago, IL, USA, ² Northwestern University, Evanston, IL, USA

Background, Motivation and Objective

The functional role and structure of some biological tissues, such as skeletal muscle, results in anisotropy in both material properties and imposed stresses. Dynamic elastography reconstruction methods for estimating soft tissue viscoelastic properties that are rooted in assumptions of isotropy and bulk wave motion may produce inaccurate estimates. The superposition of transverse isotropy in material properties and axially-aligned prestress due to passive stretch or muscle activation makes it difficult to independently discern what part of the apparent anisotropy is due to material versus stress field anisotropy. Separation of this could have clinical value in that it would differentiate changes in muscle tissue structure versus muscle loading conditions. The significance of this confounding condition and strategies for decoupling material and stress-based anisotropy are investigated with a series of numerical finite element analysis (FEA) and experimental elastography studies using scanning laser Doppler vibrometry (SLDV).

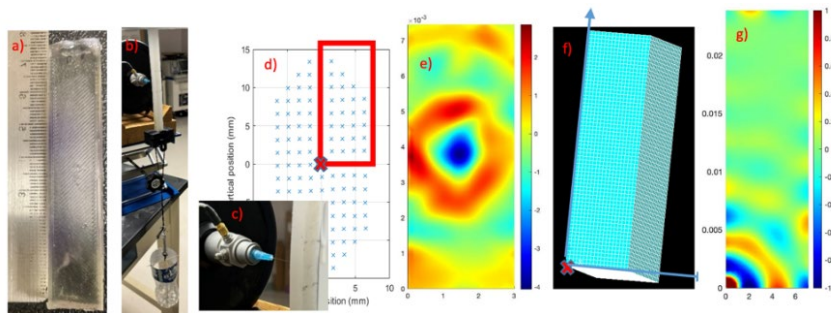
Statement of Contribution/Methods

For post-processing reconstruction of the acquired frequency response, direct Hermholtz Inversion was combined with a novel dimensional distortion approach – transformation acoustoelastography (TAE) – to independently estimate complex shear modulus, shear anisotropic ratio, and the tensile prestress.

Results/Discussion

Studies provide a quantitative snapshot of how both anisotropic material properties and anisotropic stress fields affect the apparent shear moduli of the material.

Figure 1. a) Transverse isotropic phantom; b) Suspended and preloaded; c) Close-up of needle excitation; d) Grid points for experimental SLDV (red block shows quadrant to compare with FEA); e) Snapshot of measured waves at 1500 Hz for isotropic phantom, no prestress; f) FEA model (quarter due to symmetry); g) Snapshot of FEA-simulated wave field at 1500 Hz for unstressed isotropic phantom.



Conclusions

An elastography reconstruction approach to decouple material anisotropy from stress field anisotropy is evaluated through numerical studies and applied to experimental data, quantifying the non-negligible contributions of both material and stress field anisotropy.

Quantitative Resolution of Dynamic OCE in the Cornea: Can Wave Guidance Be Overcome?

Gabriel Regnault ¹, Agathe Marmin ², Matt O'Donnell ², Ruikang K. Wang ², Ivan (Vanya) Pelivanov ²

¹ Univ Lyon, Université Claude Bernard Lyon 1, France

² Department of Bioengineering, University of Washington, USA

Background, Motivation, and Objective

Several OCE approaches and many studies have focused on the evaluation of corneal elasticity during the last decade. However, quantification of localized changes in elasticity is still out of reach which is mainly due to the complexity of the corneal structure. Indeed, the cornea represents a layer of highly organized collagen fibers (lamellae) running in-plane thorough the stroma with quasi-random orientation but not out of plane, introducing strong asymmetric mechanical bounding and anisotropy. This results in the fact that the propagation of mechanical waves in the cornea is guided and is defined by corneal thickness and at least 2 shear moduli. An ultimate resolution at which corneal elastic moduli can still be reconstructed correctly (i.e. quantitative resolution) with wave-based OCE is hereby not a trivial subject.

Statement of Contribution/Methods

This talk will summarize results attempts of spatially resolved reconstructing corneal anisotropic mechanical moduli and determines the ultimate in-plane and in-depth resolution which can be reached independently of how mechanical waves were generated and detected.

Result/Discussion

Our results are based on comprehensive theoretical analysis in frames of a nearly-incompressible transverse isotropic (NITI) model, numerical simulations in OnScale and experimental studies using acoustic micro-tapping OCE. Different wave-excitation and detection schemes are considered including pump-probe (with both single-frequency and broadband excitations) and reverberant methods.

Conclusions

We clearly show that wave-guidance is the main factor determining both in-depth and in-plane resolution in the dynamic OCE, again, independently of the wave excitation and detection methods. Individual corneal layers can be resolved only if their structure is known, and a proper multi-layer model is used for reconstruction. Resolution of only two corneal layers (following corneal crosslinking) has been demonstrated so far. Laterally, we claim that the resolution cannot be better than 2 times of the corneal thickness for both mechanical moduli. We hope that this study will improve understanding about what can be ultimately done, reduce speculation and allow critically evaluate results claiming super-resolution achieved in the corneal OCE.

Improving Shear Wave Elastography by Coded Acoustic Radiation Force

Enrique González-Mateo¹, Matthew W. Urban², Noé Jiménez

¹ Instituto de Instrumentación para Imagen Molecular (I3M), CSIC - Universitat Politècnica de València, València, Spain

² Department of Radiology, Mayo Clinic, Rochester, MN, USA

Background, Motivation and Objective

Shear wave elastography (SWE) is widely used for assessing tissue stiffness but is limited by low shear wave (SW) amplitudes and signal-to-noise ratio (SNR). We propose a pulse compression-based excitation method using maximum length sequences (MLS) to enhance SW magnitude while ensuring safety levels.

Statement of Contribution/Methods

A coded acoustic radiation force (ARF) method was implemented on a Verasonics system, integrating MLS-based pulse compression to boost shear wave energy. The method was validated in elastic and viscoelastic phantoms, *ex vivo* porcine muscle, *in vivo* human biceps and human arterial tissue. Key metrics analyzed included SNR, group and phase velocity estimations, and acoustic safety parameters.

Results/Discussion

The coded ARF method improved SNR by 6–8 dB across different media and tissues, enabling more accurate velocity estimation. Additionally, it allowed a 40% reduction in the mechanical index (MI) while maintaining comparable SNR. The method also showed robust performance in dynamic environments, including *in vivo* arterial imaging, improving reliability in motion-prone applications.

Conclusions

Pulse compression-based SWE improves imaging quality while reducing mechanical stress, enabling safer applications in fragile tissues like lungs and neonates. Its robustness against motion artifacts expands the potential for arterial and cardiovascular elastography, broadening the clinical reach of SWE.

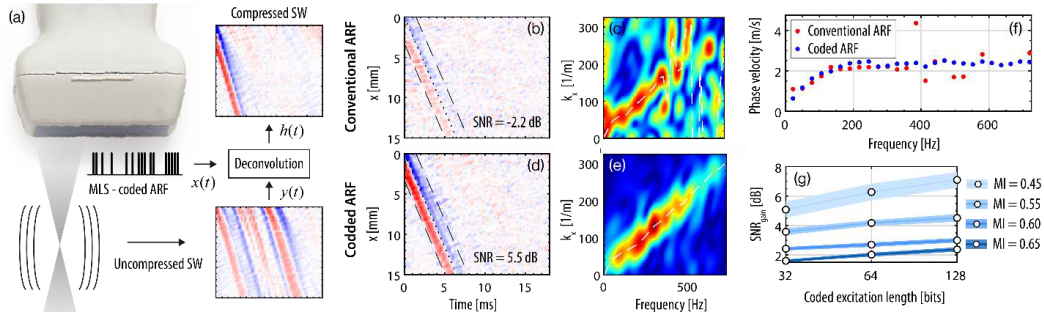


Figure 1. Schematic of the method (a), where the coded ARF input $x(t)$ generates the decompressed shear wave $y(t)$, used to compute the compressed signal $h(t)$ via deconvolution. Wave propagation in time (b, d) and frequency (c, e) for conventional and coded ARF, with phase velocity curves (f). Finally, the SNR gain is plotted across voltages and excitation lengths (g).

Ultrasound Time-Harmonic Elastography in Adult Zebrafish

Mareike Wolff¹, Tom Meyer², Jakob Jordan², Julia Köppke¹, Anja I.H. Hagemann¹, Inqolf Sack²

¹ Department of Pediatric Oncology/Hematology, Charité–Universitätsmedizin, Berlin, Germany.

² Department of Radiology, Charité – Universitätsmedizin, Berlin, Germany.

Background, Motivation and Objective

The zebrafish is an important preclinical model in medical research, particularly in oncology. Current methods for studying viscoelastic properties of adult zebrafish are limited to *ex vivo* techniques like high resolution MRE or cannot achieve sufficiently high resolution to differentiate anatomical details. Here we use ultrasound time-harmonic elastography (THE), which enables fast, high-resolution measurement of mechanical properties in live adult zebrafish.

Statement of Contribution/Methods

Ultrasound measurements were performed with a VisualSonics Vevo2100 preclinical scanner and a MS550D linear transducer of 40 MHz center frequency and 100Hz frame rate. Multifrequency vibrations (1028, 1120, 1232, 1324, 1444, 1536 Hz) were applied ventrally to the fish by a loudspeaker (Fig. 1a). *k*-MDEV gradient inversion was employed to generate shear-wave-speed (SWS) maps as a proxy of stiffness.

Results/Discussion

B-mode images and SWS maps were successfully obtained within the whole field-of-view and with sufficient spatial resolution to differentiate between anatomical regions within the zebrafish (Fig. 1 B, C, D), enabling the analysis of stiffness across different organs.

Conclusions

In this study, we have successfully established a novel approach to measure the mechanical properties of live adult zebrafish. By providing high spatial and temporal resolution, our setup could enable real-time, non-invasive monitoring of zebrafish under anesthesia, thus opening new avenues for the *in vivo* study of tumor biology and disease progression.

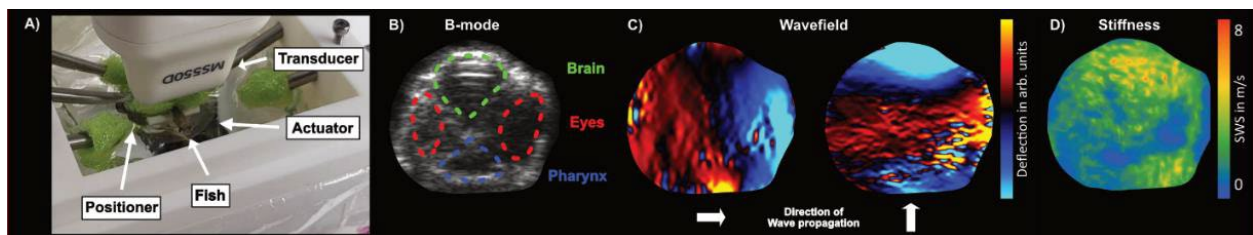


Figure 1. (A) Experimental setup: The zebrafish is secured in a water-filled basin using sponges and placed on a loudspeaker. The ultrasound probe captures images in sagittal or transverse sections. (B) B-mode image showing a transverse section of the zebrafish for anatomical overview. (C) Wavefield of the same section, shown in horizontal and vertical directions. (D) Resulting SWS map.